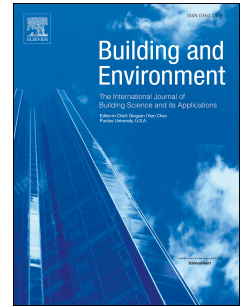


Journal Pre-proof

Probable airborne transmission of SARS-CoV-2 in a poorly ventilated restaurant

Yuguo Li, Hua Qian, Jian Hang, Xuguang Chen, Pan Cheng, Hong Ling, Shengqi Wang, Peng Liang, Jiansen Li, Shenglan Xiao, Jianjian Wei, Li Liu, Benjamin J. Cowling, Min Kang



PII: S0360-1323(21)00195-5

DOI: <https://doi.org/10.1016/j.buildenv.2021.107788>

Reference: BAE 107788

To appear in: *Building and Environment*

Received Date: 1 February 2021

Revised Date: 5 March 2021

Accepted Date: 6 March 2021

Please cite this article as: Li Y, Qian H, Hang J, Chen X, Cheng P, Ling H, Wang S, Liang P, Li J, Xiao S, Wei J, Liu L, Cowling BJ, Kang M, Probable airborne transmission of SARS-CoV-2 in a poorly ventilated restaurant, *Building and Environment* (2021), doi: <https://doi.org/10.1016/j.buildenv.2021.107788>.

This is a PDF file of an article that has undergone enhancements after acceptance, such as the addition of a cover page and metadata, and formatting for readability, but it is not yet the definitive version of record. This version will undergo additional copyediting, typesetting and review before it is published in its final form, but we are providing this version to give early visibility of the article. Please note that, during the production process, errors may be discovered which could affect the content, and all legal disclaimers that apply to the journal pertain.

© 2021 Published by Elsevier Ltd.

1 **Running title: Airborne transmission of SARS-CoV-2**

2
3 **Probable airborne transmission of SARS-CoV-2 in a poorly ventilated**
4 **restaurant**

5
6 Yuguo Li ^{a, h, †}, Hua Qian ^{b, †}, Jian Hang ^{c, †}, Xuguang Chen ^d, Pan Cheng ^a, Hong Ling ^c,
7 Shengqi Wang ^b, Peng Liang ^e, Jiansen Li ^d, Shenglan Xiao ^{a, i}, Jianjian Wei ^f, Li Liu ^g,
8 Benjamin J. Cowling ^h, and Min Kang ^{d, *, †}

9
10 ^a Department of Mechanical Engineering, The University of Hong Kong, Hong Kong, China

11 ^b School of Energy and Environment, Southeast University, Nanjing, China

12 ^c School of Atmospheric Sciences, Sun Yat-sen University, Guangzhou, China

13 ^d Guangdong Provincial Center for Disease Control and Prevention, Guangzhou, China

14 ^e Guangdong Field Epidemiology Training Program, Ganzi Tibetan Autonomous Prefecture
15 Center for Disease Control and Prevention, Sichuan, China

16 ^f Institute of Refrigeration and Cryogenics and Key Laboratory of Refrigeration and
17 Cryogenic Technology of Zhejiang Province, Zhejiang University, Hangzhou, China

18 ^g School of Architecture, Tsinghua University, Beijing, China

19 ^h School of Public Health, The University of Hong Kong, Hong Kong, China

20 ⁱ School of Public Health, Sun Yat-sen University, Shenzhen, China (Present address)

21 [†] These authors contributed equally

22
23 ^{*} Corresponding author:

24 Mr. Min Kang

25 Guangdong Provincial Center for Disease Control and Prevention

26 No.160 Qunxian Road, Panyu District, Guangzhou, Guangdong, P. R. China, 511430

27 E-mail: kangmin@cdcp.org.cn, Tel.: +86 20 31051456, Fax: +86 20 31051191

30 **Highlights**

31

32 This outbreak involved ten infected persons in three families;

33

34 Full video recording at time of infection allows restoration of the scene;

35

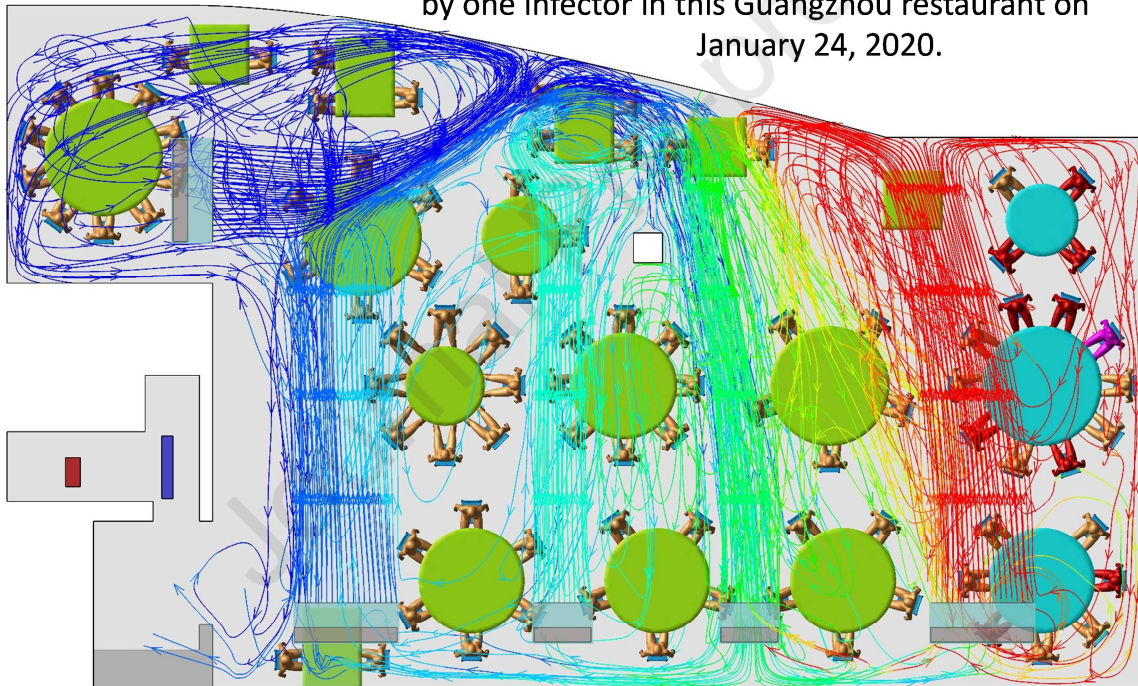
36 Time-averaged ventilation rates were only 0.9 L/s per person in the restaurant;

37 Insufficient ventilation played a role in this outbreak of COVID-19.

38

39 **Graphical abstract (Color Online)**

Poor ventilation and air circulation probably led to COVID-19 infection of 9 patrons
by one infector in this Guangzhou restaurant on
January 24, 2020.



40

41

42

43 Abstract

44 Although airborne transmission of severe acute respiratory syndrome coronavirus 2 (SARS-
45 CoV-2) has been recognized, the condition of ventilation for its occurrence is still being
46 debated. We analyzed a coronavirus disease 2019 (COVID-19) outbreak involving three
47 families in a restaurant in Guangzhou, China, assessed the possibility of airborne
48 transmission, and characterized the associated environmental conditions. We collected
49 epidemiological data, obtained a full video recording and seating records from the restaurant,
50 and measured the dispersion of a warm tracer gas as a surrogate for exhaled droplets from the
51 index case. Computer simulations were performed to simulate the spread of fine exhaled
52 droplets. We compared the in-room location of subsequently infected cases and spread of the
53 simulated virus-laden aerosol tracer. The ventilation rate was measured using the tracer gas
54 concentration decay method. This outbreak involved ten infected persons in three families (A,
55 B, C). All ten persons ate lunch at three neighboring tables at the same restaurant on January
56 24, 2020. None of the restaurant staff or the 68 patrons at the other 15 tables became infected.
57 During this occasion, the measured ventilation rate was 0.9 L/s per person. No close contact
58 or fomite contact was identified, aside from back-to-back sitting in some cases. Analysis of
59 the airflow dynamics indicates that the infection distribution is consistent with a spread
60 pattern representative of long-range transmission of exhaled virus-laden aerosols. Airborne
61 transmission of the SARS-CoV-2 virus is possible in crowded space with a ventilation rate of
62 1 L/s per person.

63 **Keywords:** COVID-19, SARS-CoV-2, airborne transmission, aerosol transmission, building
64 ventilation

65

66 **1. Introduction**

67 Following a debate of airborne transmission of SARS-CoV-2 (Morawska and Cao, 2020), the
68 virus that causes COVID-19, in the continuing COVID-19 pandemic, leading health
69 authorities have recognized the importance of airborne transmission in special settings since
70 October 2020 (US CDC, 2020; WHO, 2020). The well-known Wells-Riley equation (Riley et
71 al. 1978) suggests the importance of sufficient building ventilation in diluting the infectious
72 aerosols. However, the effective minimum ventilation rate for avoiding airborne transmission
73 remains unknown. Existing ventilation standards such as ASHRAE 62.1 (2019) do not
74 consider infection control as their objectives. The Wells-Riley equation or its variants may
75 be used to determine the minimum ventilation rate if the quanta generation rate is known,
76 however, significant uncertainty exists in the existing available quanta generation data for
77 COVID-19 (Buonanno et al. 2020; Dai and Zhao, 2020; Miller et al. 2021). Measurement of
78 ventilation rates in the infection venue of an outbreak has been challenging due to difficulties
79 in identification of an airborne outbreak, and difficulties in immediate access to infection
80 venue and data availability of infectors and susceptible in infection venue at the time of
81 infection.

82 Here we report a detailed epidemiological and environmental study of a restaurant outbreak
83 in Guangzhou, China. The COVID-19 outbreak was identified in early 2020 and linked to
84 three seemingly non-associated clusters of unrelated families (A, B, C) (Lu et al. 2020).
85 Families B ($n = 4$) and C ($n = 7$) comprised local Guangzhou residents with no history of
86 travel to or encounters with inhabitants from Hubei, but nevertheless three members of family
87 B and two members of family C were confirmed to be infected with SARS-CoV-2 on
88 February 4 or 6, at which time only 322 cases of infection (98 local cases and 224 imported
89 cases) had been confirmed in the city of nearly 13 million residents.

90 Local health officials learned that families B and C had eaten lunch at the same restaurant on
91 Chinese New Year's Eve (January 24, 2020), as had family A ($n = 10$) from Wuchang,
92 Wuhan (the epicenter of the Chinese epidemic), who had arrived in Guangdong by train on
93 January 23. One person from family A reported experiencing the onset of COVID-19
94 symptoms on January 24, and video records from the restaurant show that families A, B, and
95 C were seated at tables along the exterior window, with family A's table in the center. None
96 of the restaurant waiters or remaining 68 patrons distributed at 15 other tables became
97 infected with SARS-CoV-2. Families A, B, and C had not met previously and did not have
98 close contact during the lunch, aside from some patrons sitting back-to-back.

99 Our field measurement of ventilation was performed in the restaurant with the original table
100 setup on March 19–20. To investigate the possibility of airborne transmission of SARS-CoV-
101 2, we also analyzed the spatial distribution data from this outbreak using computational fluid
102 dynamics (CFD) simulations. We use our results to assess the ventilation conditions of
103 airborne transmission.

104 **2. Methods**

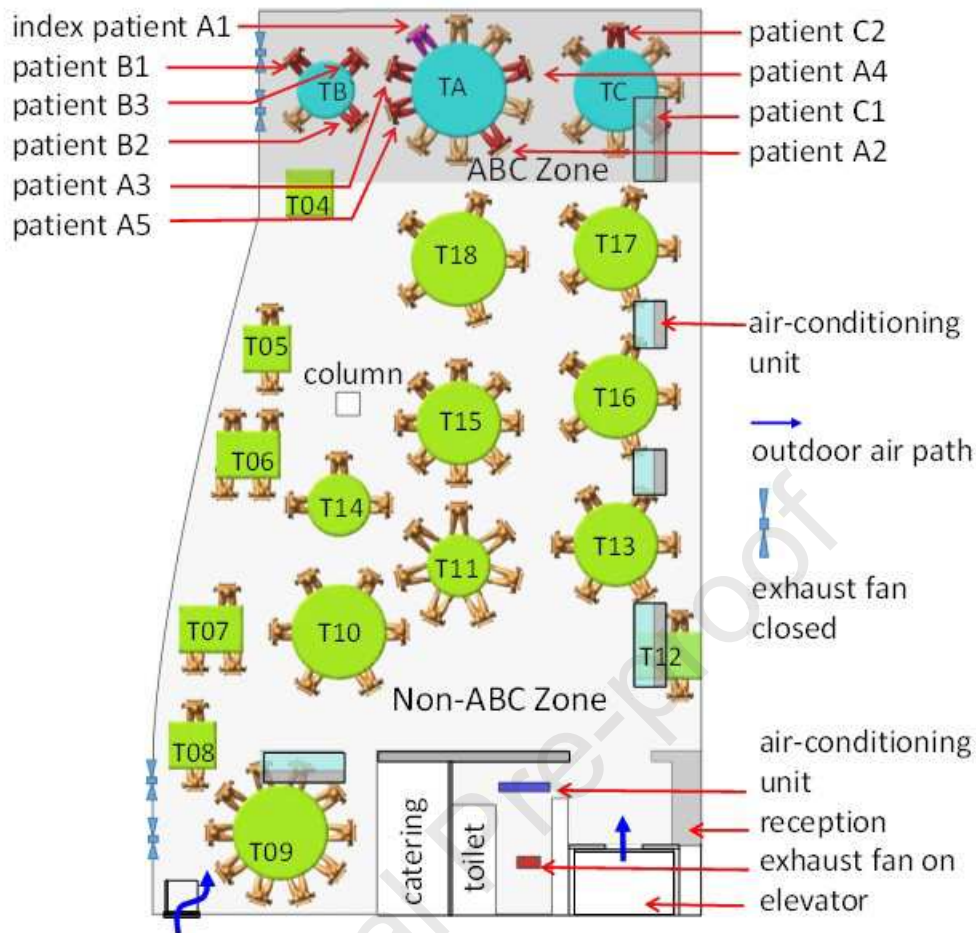
105 **2.1. Epidemiologic analysis**

106 We obtained the seating arrangement of the three family members and remaining patrons in
107 Restaurant X as well as the dates of COVID-19 symptom onset, where the symptom onset
108 date is defined as the day when symptoms (e.g., fever or cough) were first noticed by the
109 patient. SARS-CoV-2 infection was confirmed by real-time polymerase chain reaction with
110 reverse transcription (RT-PCR) analysis of throat swabs. Demographic data, travel history,
111 exposure history, and symptoms of the infected individuals were collected (Lu et al. 2020).
112 We also obtained the floor plan and design of the air conditioning and ventilation system of
113 the restaurant, and the hourly weather data for January 24 from a weather station near the site.

114 Full closed-circuit television camera records of the restaurant and elevator were reviewed to
115 determine the elevator use by patrons, the fire-door use by both patrons and waiters, the table
116 and seating arrangement during the lunch, and any close contact behavior between Family A
117 and others.

118 Restaurant X has five floors. The outbreak occurred on the third floor, which has a volume of
119 431 m^3 (height of 3.14 m, length of 17 m, and average width of 8.1 m) (Figure 1). Large and
120 small tables have a diameter of 1.8 m and 1.2 m, respectively, and rectangular tables measure
121 $0.9 \text{ m} \times 0.9 \text{ m}$ and $1.2 \text{ m} \times 0.9 \text{ m}$. Five fan coil air-conditioning units are installed on the third
122 floor, and there is no outdoor air supply: ventilation is thus achieved using only infiltration
123 and natural ventilation through an occasionally open door driven by buoyancy forces and an
124 exhaust fan installed inside the restroom. Four exhaust fans are installed on the south glass
125 window but were not used during this lunch. At noon on January 24, the third floor of the
126 restaurant had 18 tables and 89 patrons. We label tables A, B, and C as TA, TB, and TC,
127 respectively, and the remaining tables are labeled as T4–T18 (Figure 1). According to video
128 analyses, the fire door was used approximately every 2 min.

129



130

131 **Figure 1.** (Color Online) Distribution of SARS-CoV-2 infection cases at tables in Restaurant
 132 X. The probable air-flow zones are shown in dark grey and light grey. Eighty-nine patrons
 133 are shown at the 18 tables, with one table being empty (T04). Tables TA, TB, and TC are
 134 where families A, B, and C sat, some of whose members became infected. Patient A1 at TA
 135 is the suspected index case, who had symptoms shortly after returning to the hotel where
 136 Family A was staying. Patients A2–A5, B1–B3, and C1–C2 are the individuals who became
 137 infected. Other tables are numbered as T04–T18. Each of the five air-conditioning units (fan
 138 coil units) condition a particular zone. Patrons and waiters entered the restaurant floor via the
 139 elevator and stairwell, which are connected by the fire door.

140

141 We studied the infection data with regards to seating location and used a chi-square test to
142 explore the association between a patron's location (i.e., table) and his/her probability of
143 becoming infected. Table A was excluded in this analysis. The other tables were categorized
144 according to two criteria: distance from TA (e.g., immediate vs. remote neighbors) and air-
145 conditioning zone. The ABC zone was that immediately around TA, TB, and TC and
146 serviced by one air conditioning unit, and the non-ABC zone was everywhere else, serviced
147 by the four other air conditioning units.

148 **2.2. Experimental tracer gas measurements and computational fluid-dynamics** 149 **simulations**

150 Tracer gas measurements and computational fluid dynamics (CFD) simulations were used to
151 predict the spread of fine droplets exhaled by the index case and the detailed airflow pattern
152 in the restaurant. The CFD simulation models were the same as those used in previous studies
153 of two 2003 Severe Acute Respiratory Syndrome coronavirus (SARS-CoV) outbreaks in
154 Hong Kong (Li et al. 2005; Wong et al. 2004; Yu et al. 2004).

155 The tracer measurement was carried out on March 19–20 when the intensity of the direct
156 solar radiation was similar to that on January 24, i.e., weak sunshine, with clouds and rain.
157 We first measured the supply/return/exhaust air flow and temperature at each air-conditioning
158 unit and at the exhaust fan in the restroom. We arranged the tables and chairs to match the
159 arrangement used at the January 24 lunch, as determined by the video analyses. The air
160 conditioning units were turned on and the exhaust fans in the vertical glass window were left
161 off to simulate the air-flow conditions at the time of SARS-CoV-2 infection during the lunch
162 on January 24. Volunteers were not recruited because the experiment was performed during
163 the strict intervention (i.e., partial lockdown) phase of the epidemic in Guangzhou. However,
164 nine of our team members volunteered to sit at tables A, B, and C and simple thermal
165 mannequins were placed at the others. The mannequins were warm and hollow, containing a

166 60-W electrical bulb enclosed by a stainless steel cylinder, which produced warm plumes
167 similar to those produced by the human volunteers. A 60-W electrical bulb was also used to
168 simulate warm food on each table.

169 The tracer gas measurement consisted of two stages. In the first stage, we released ethane gas
170 through an 8-mm inner diameter pipe at a speed of 1.5 m/s at 32–34 °C, with the pipe outlet
171 placed immediately above the index case's nose. This mode of release mimicked the index
172 case (assumed to be A1) talking and moving their head around. Tracer gas is known to be an
173 effective surrogate for modeling the spread of fine droplets or droplet nuclei (Bivolarova et al.
174 2017). In the first of two experiments, we monitored the gas concentrations at 14 points,
175 namely all of the chairs where the infected members of families B and C had sat (Figure C.1).
176 In the second experiment, gas concentrations were only monitored at seven points, owing to
177 the time required for rotational sampling at each point.

178 In the second stage, the ventilation rate was measured using the tracer concentration decay
179 method, which involved the release of a tracer gas into the restaurant and subsequent mixing
180 with the flow from 10 desk fans. We measured the tracer concentration at three points in the
181 room. The elevator and fire door were opened every 2 min to mimic the traffic that was
182 observed in the recording of the January 24 lunch, with the fire door closing automatically
183 after a period of 3 s. We identified an exhaust flow through the doorway of the restroom and
184 bidirectional air exchange through the opening and closing of the fire door. The non-
185 operating exhaust fans were sealed relatively well, with nearly negligible air flow. After the
186 measurements, we assigned the health status (ill vs. healthy) of each person at non-A tables
187 as the dependent variable and applied a binary logistic regression model to investigate the
188 association between the measured concentrations of tracer gas and infection probability.

189 We adopted the widely used CFD software package Fluent (Ansys Fluent, USA), which is a
190 three-dimensional, general-purpose CFD software package for modeling fluid flows. We used

191 the basic renormalization-group (RNG) k - ε turbulence model to simulate the effects of
192 turbulence on airflow and dispersion of pollutants. We assumed that the virus-laden water
193 droplets generated from the index case at TA rapidly evaporated (i.e., after a few s in air). We
194 first approximated the exhaled droplet nuclei as a passive scalar, as in the experiments, and
195 the deposition effect was therefore neglected. The prediction was then compared to the
196 measured value. Next, we considered the deposition of droplet nuclei (using a drift-flux
197 model of Holmberg and Li , 1998), filtration of the air conditioning units (with a filtration
198 efficiency of 20% following a preliminary measurement on site), and deactivation of the virus
199 in aerosols (Van Doremalen et al. 2020), and predicted the temporal concentration profiles of
200 the droplet nuclei containing the virus, which was then used to calculate the total exposure at
201 each table. Only a representative droplet nuclei size of 5 μm is modeled, and its surface
202 deposition was ignored as the deposition loss of fine droplet nuclei is significantly small
203 compared to virus deactivation (Miller et al. 2021). After CFD modeling, we used the health
204 status (ill vs. healthy) of each person at non-A tables as the dependent variable and applied a
205 binary logistic regression model to investigate the association between the predicted
206 concentration of tracer gas and predicted exposure to droplet nuclei and infection probability.

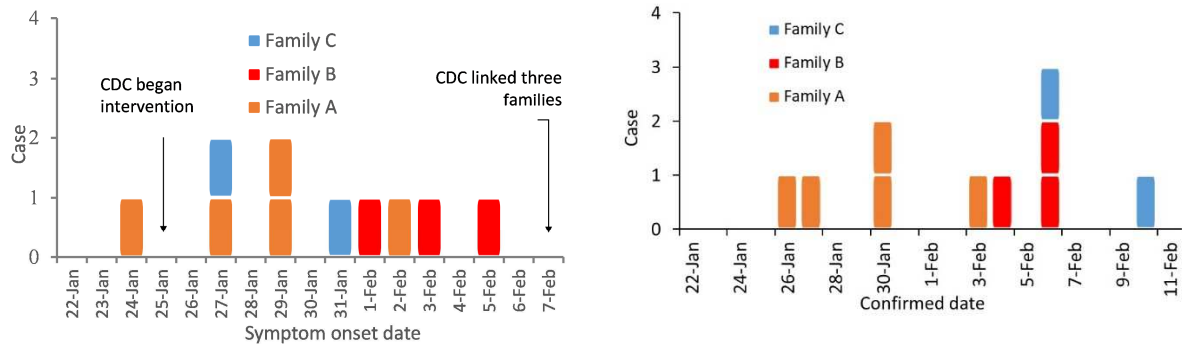
207 **3. Results**

208 **3.1. The outbreak**

209 Detailed epidemiological, clinical, laboratory, and genomic findings for this outbreak and all
210 of the associated patients have been described in detail by Lu et al. (2020). The first
211 confirmed case (A1) from family A, who was confirmed on January 24, is assumed to be the
212 index case (Figure 1). Patient A1 first had symptoms of a fever and cough in the late
213 afternoon of January 24 (Figure 2A, Table A.1). The last patient was confirmed on February
214 6 (Figure 2B). The three families occupied the restaurant at different times (family A 12:01–
215 13:23; family B 11:37–12:54; and family C 12:03–13:18). According to the video analysis,

216 there was no significant close contact between the three families in the elevator or restroom
217 (Supplementary information B). Contact tracing identified 68 patrons on the third floor at the
218 same time as families A, B, and C, and 102 patrons on other floors. We also identified 57
219 workers in the restaurant including 8 on the third floor, a taxi driver who had A1 as a
220 customer on the afternoon of January 24, and 11 workers in the hotel where family A stayed.
221 The hotel is within walking distance of the restaurant. All of these close contacts were
222 identified after February 7. Only 11 non-infected members of families A, B, and C were
223 quarantined in a central facility; throat swab samples were taken but yielded negative results
224 for SARS-CoV-2. The 8 restaurant workers on the third floor, 11 hotel workers, and 19
225 patrons at other third-floor tables were home quarantined for 14 days and their symptoms
226 were continuously monitored. The remaining identified contacts were only followed up by
227 telephone and none reported any symptoms. Thus, only the 10 patrons in the restaurant were
228 infected, comprising the index case and nine others, including the five members of families B
229 and C who are assumed to have been infected at this lunch due to exposure to exhaled
230 droplets from the index case that contained virus particles. Families B and C had no close
231 contact with any known COVID-19 patients and/or visitors from Hubei Province 14 days
232 prior to the onset of their symptoms (Figure D.1). Although various scenarios of transmission
233 are possible (e.g., C2 may have become infected while caring for C1), Lu et al (2020)
234 determined that at least one member from both families B and C was exposed to SARS-CoV-
235 2 at the restaurant.

236



(A)

(B)

237 **Figure 2.** (Color Online) Dates of (A) symptom onset and (B) confirmation of the 10 patients
 238 from the three families. Patients from family A, B, C are represented by yellow, red and blue
 239 squares respectively.

240 The arrival and departure times of patrons at all tables are listed in Table 1. Upon arriving at
 241 the restaurant, families A, B, and C took the elevator to the third floor and did not remain in
 242 the reception area, as they had previously booked tables. Family A used the elevator in two
 243 groups. One patron from T18 shared the lift with the first group. The second comprised the
 244 remaining two members of family A. Families B and C and patient C1 used the elevator
 245 separately.

246 Shortly after being seated, patient A4 and two unaffected females of family A left their table
 247 to use the restroom. During the meal, patient A4 left the table two additional times to go to
 248 the catering room to retrieve new chopsticks or a spoon. An unaffected male member of
 249 family C used the restroom shortly after sitting down and overlapped there for 1 min with
 250 three members of family A. Some members of the three families used the restroom
 251 immediately prior to leaving the restaurant. No sharing of items (e.g., a kettle) was observed
 252 between the three tables and no conversations occurred between the three families. During

253 the meal, the patrons at TA were active, with instances of members standing up and talking to
 254 the left and right, whereas patrons at TB and TC were comparatively inactive.

255 **Table 1** Arrival, departure, and overlap time.

Table	Arrival (first patron at table)	Departure	Lunch duration (min)	Starting exposure	Overlap with Table A (min)	Total exposure time (min)	Period of exposure after Table A's departure (min)
TA	12:01	13:23	82	12:01	82	82	0
TB	11:37	12:54	77	12:01	53	53	0
TC	12:03	13:18	75	13:00	75	77	0
T05	11:32	12:53	81	12:01	52	52	0
T06	11:36	13:23	107	12:01	82	82	0
T07	11:29	13:10	101	12:01	69	69	0
T08	12:28	13:37	69	12:28	55	69	14
T09	11:47	13:16	89	12:01	75	75	0
T10	11:07	13:28	141	12:01	82	82	5
T11	11:32	13:11	99	12:01	70	70	0
T12	12:13	13:17	64	12:13	64	64	0
T13	11:53	12:51	58	12:01	50	50	0
T14	11:23	13:02	99	12:01	61	61	0
T15	11:55	13:30	95	12:01	82	89	7
T16	11:24	12:49	85	12:01	48	48	0
T17	13:00	14:19	79	13:00	23	79	56

T18	11:34	13:18	104	12:01	77	77	0
-----	-------	-------	-----	-------	----	----	---

256

257

258 3.2. Spatial distribution analysis of infection cases

259 The tables and patrons were first categorized by distance from TA, as immediate neighbors
 260 (TB, TC, and T18) or remote neighbors (tables T4–17). The 10 patients who were shortly
 261 thereafter confirmed as having COVID-19 sat at one of the three tables by the window. Three
 262 of the four members of family B were infected, and two of the seven members of family C
 263 were infected. Five members of family A were also infected, including the index case. The
 264 two patrons at TC who sat the closest to TA were not infected, nor were any patrons at the
 265 remote neighboring tables, but the patrons at neighboring tables had a higher infection
 266 probability than patrons at remote tables ($\chi^2 = 16.08$, $P < 0.001$, chi-squared test with
 267 continuity correction, Table 2). The infection risk was also higher for patrons at zone-ABC
 268 tables than those at non-ABC zone tables ($\chi^2 = 25.78$, $P < 0.001$). None of the patrons seated
 269 in the non-ABC zone were infected.

270

271 **Table 2.** Number of cases and susceptible patrons at non-A tables in different zones of

272 Restaurant X. There were a total of 79 patrons at the other 17 tables.

273

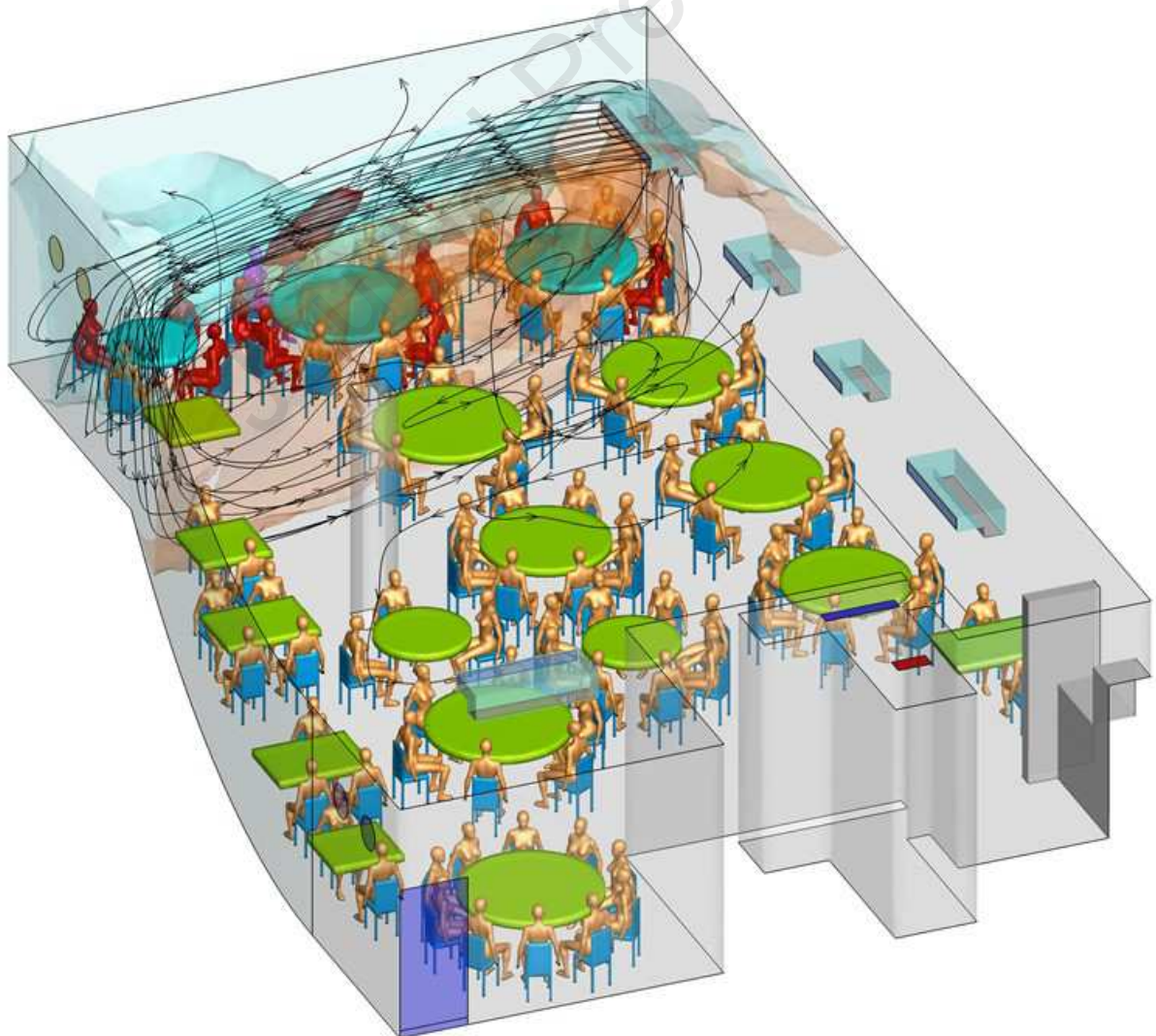
Category of zones	Zones	Number of patrons	Number of infected cases	Attack rate (%)	RD* (95% CI)	χ^2	P
Table A	Immediate neighboring	16	5	31.25	31.25	16.08 [#]	<0.001 [#]

neighbors	tables				(8.54, 53.96)		
	Remote neighboring tables	63	0	0			
Air conditioning	ABC zone	11	5	45.45	45.45	25.78 [#]	<0.001 [#]
	Non-ABC zone	68	0	0	(16.03,74.88)		

274 *RD: Rate difference

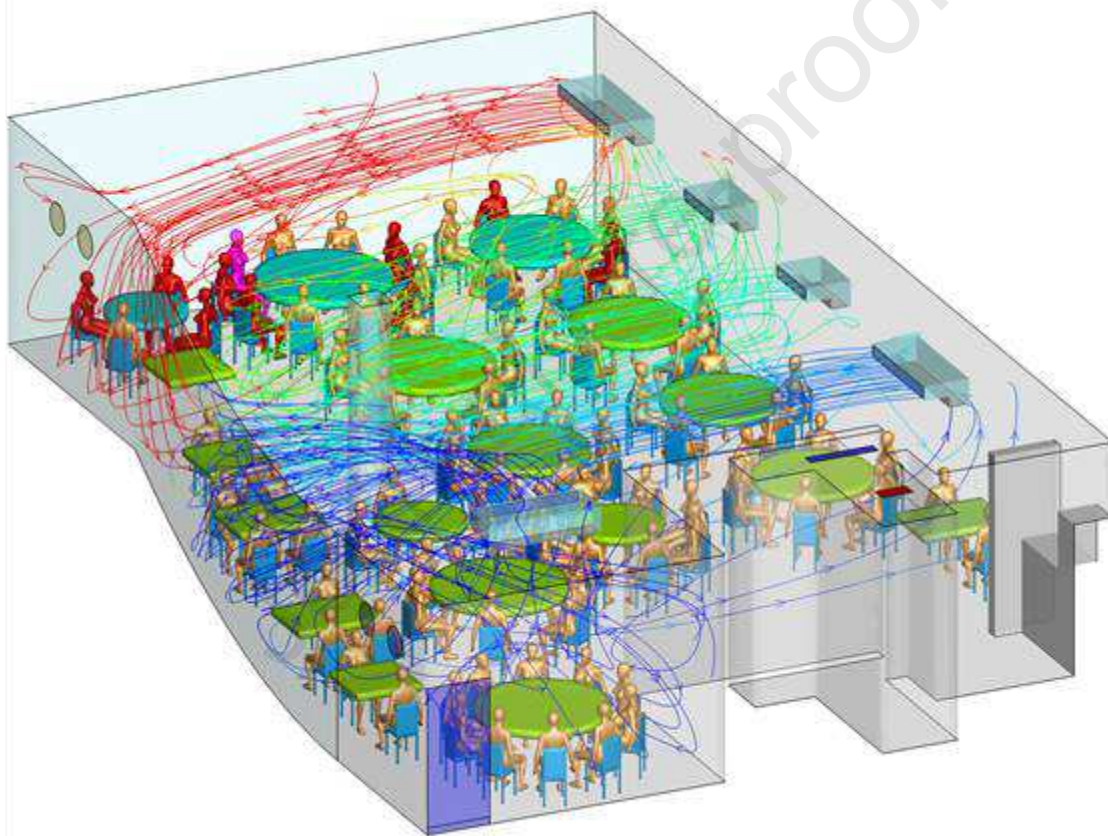
275 # Chi-squared test with continuity correction

276



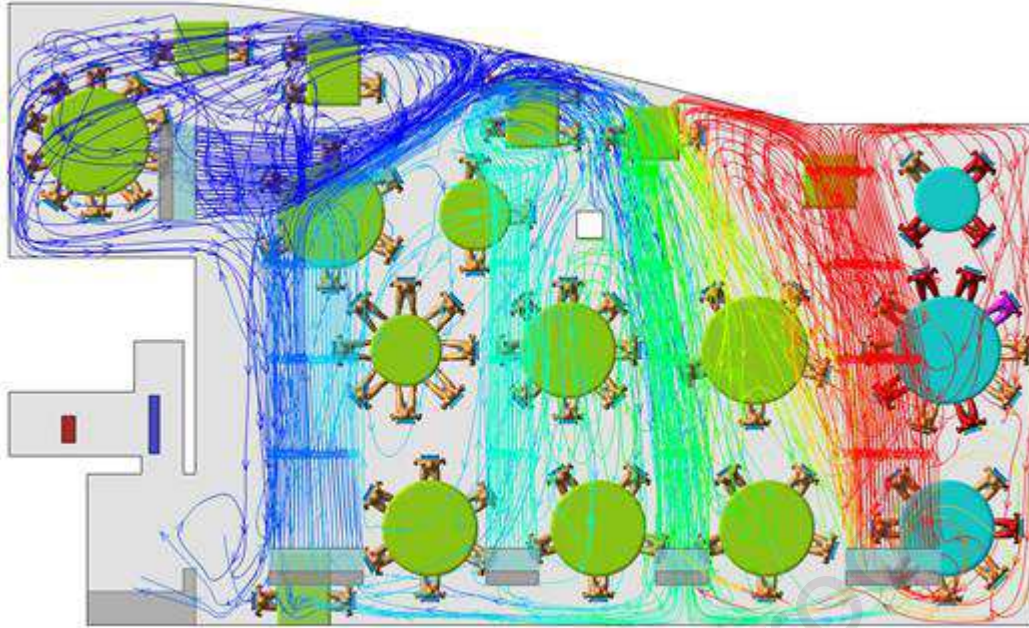
277

278 **Figure 3.** (Color Online) Simulated dispersion of fine droplets exhaled from index case A1
279 (purple), which are initially confined within the cloud envelope (ABC bubble) due to the
280 zoned air-conditioning arrangement. The fine droplets disperse into the other zone via air
281 exchange and are eventually removed via the restroom exhaust fan. The streamlines
282 originated from the ABC air conditioning unit are plotted to show the formation of the ABC
283 bubble. The ABC zone clearly has a higher concentration of fine droplets than the non-ABC
284 zone. Other infected patients are shown in red and non-infected patrons in gold.



285

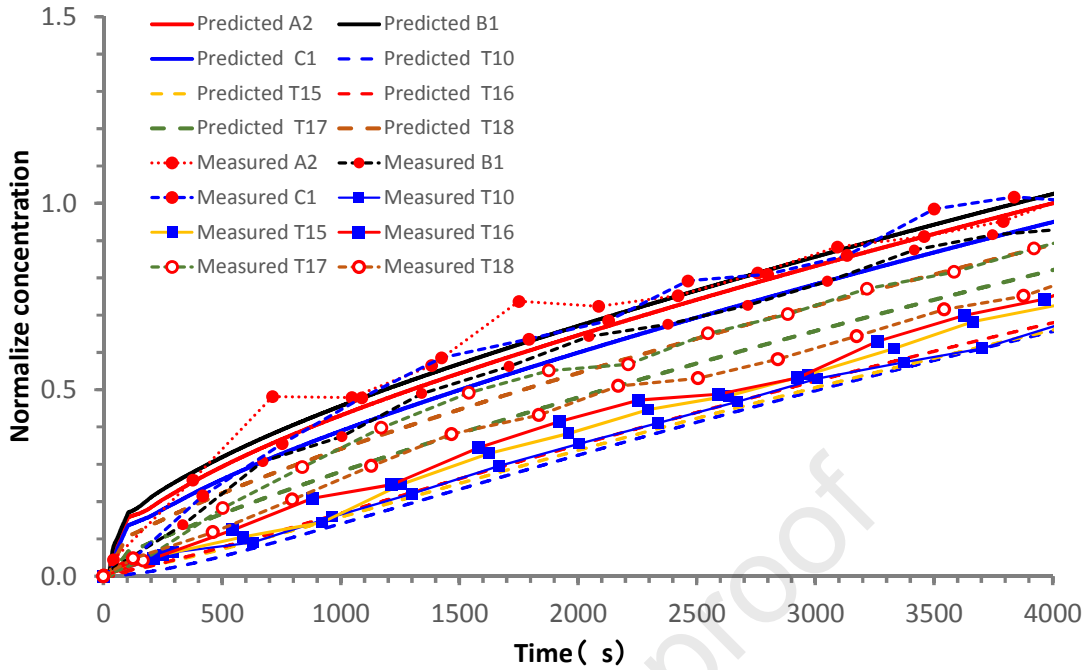
286 (A)



287

288 (B)

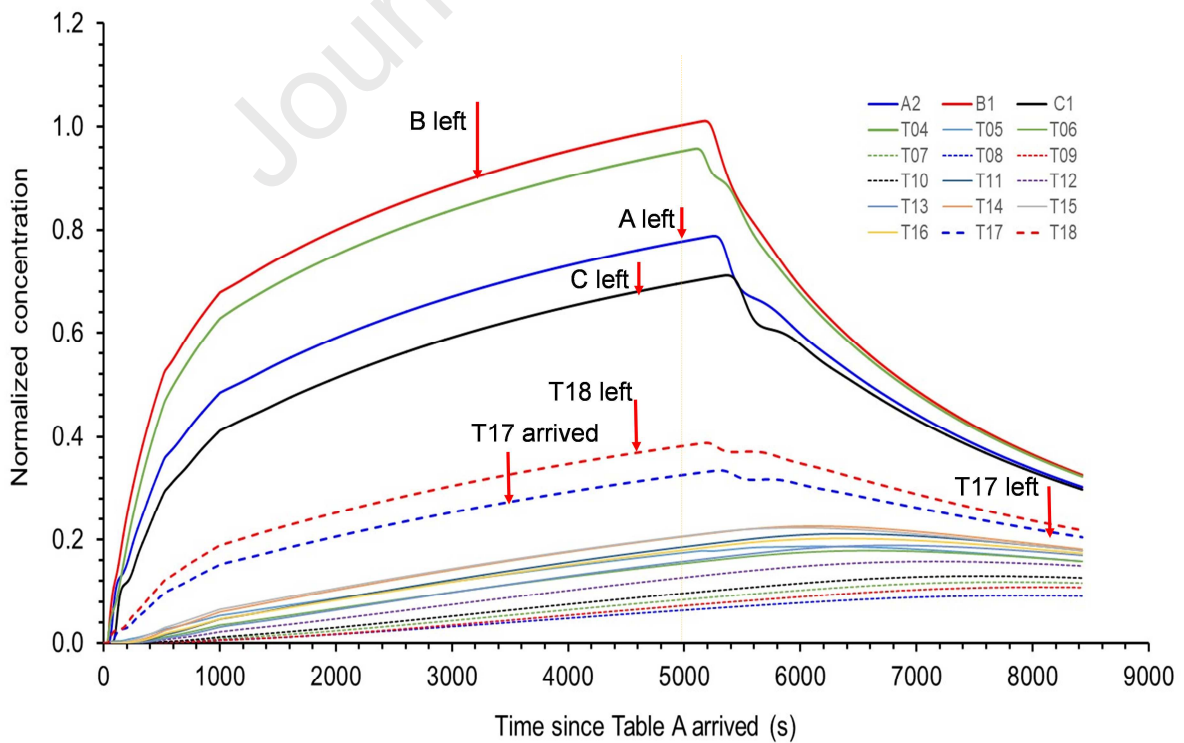
289 **Figure 4.** (Color Online) Simulated air streamlines originating from the air conditioning units
290 in the restaurant using computational fluid dynamics. The index case A1 is shown in purple,
291 other infected patients in red, and non-infected in gold. The streamlines are colored by the
292 concentration of predicted infectious droplet nuclei, with red the highest and blue the lowest.
293 (A) 3D view and (B) top view.



294

295 **Figure 5.** (Color Online) Comparison between measured and predicted concentrations at
 296 monitoring points during exhaled tracer spread test, normalized by the A2 value at 4000 s.

297



298

299 **Figure 6.** (Color Online) Predicted concentrations normalized to B1 at 4920 s for some
300 patrons at tables A, B, and C, and other tables after table A patrons arrived at time zero
301 (12:01 pm). Table A patrons left the restaurant at time 4920 s (1:22 PM). Due to the nature of
302 the air flows, the concentrations for some patrons continued to rise after 4920 s. The results
303 are used to calculate the exposure using the exposure duration data in Table 3. The prediction
304 concentration profiles clearly show a separated ABC zone (i.e., bubble, including T04, which
305 had no patrons), a T17/T18 zone, a zone with T11 and T13–16, and a zone with T07–T10 and
306 T12 close to the outdoor air supply.

307

308 **3.3. Ventilation and dispersion of exhaled droplet nuclei**

309 The results of the two tracer gas decay experiments show that the air exchange rate was only
310 0.77 air changes per hour (ACH) at 16:00–17:00 and 0.56 ACH at 18:00–19:30 (Figure C.2).
311 For a volume of 431 m³ and 89 patrons, this is equivalent to an outdoor air supply of 1.04 and
312 0.75 L/s per patron, respectively. The average measured ventilation rate is 0.9 L/s per person.
313 The predicted contaminated cloud envelope in the ABC zone is shown in Figure 3. The
314 exhaled air stream from the index case rises in the zone with families A, B, and C, following
315 the interaction of thermal plumes and the air jet of the air conditioning (Figure 4). The high-
316 momentum air-conditioning jet carries the contaminated air at ceiling height. Upon reaching
317 the opposite glass window, the jet bends downward and returns at a lower height. At each
318 table, the rising thermal plumes from the warm food and people carry the contaminated air
319 upward, and the remaining air returns to the air-conditioning unit and forms a recirculation
320 zone or bubble, referred to as the ABC zone. Similarly, other air-conditioning units also
321 produce cloud envelopes, although these are not as distinct as that in the ABC zone, due to
322 mixing by the air-conditioning jet of the air-conditioning unit above T09. Air exchange
323 occurs between all of the zones because there are no physical barriers between them. Spread

324 of exhaled droplet nuclei in the restaurant is also shown in an animation shown in Appendix
 325 B as predicted by computational fluid dynamics.

326 **Table 3.** Number of cases and susceptible patrons ($n = 89$) at the 18 different tables of
 327 Restaurant X during lunch on January 24, 2020.

Table number	Number of patrons	Number of infected	Attack rate (%)	Normalized measured tracer gas concentration	Normalized predicted tracer gas concentration	Normalized predicted exposure to droplet nuclei
TA	10	5	50.00	1.00	1.00	1.00
TB	4	3	75.00	0.87	1.04	0.76
TC	7	2	28.57	0.98	0.93	0.89
T04	0	0	NA	-	1.00	0.00
T05	2	0	0.00	-	0.62	0.07
T06	4	0	0.00	-	0.47	0.13
T07	3	0	0.00	-	0.42	0.04
T08	2	0	0.00	-	0.42	0.06
T09	10	0	0.00	-	0.32	0.04
T10	6	0	0.00	0.55	0.52	0.08
T11	7	0	0.00	-	0.57	0.12
T12	2	0	0.00	-	0.50	0.09
T13	6	0	0.00	-	0.55	0.05
T14	3	0	0.00	-	0.63	0.11
T15	8	0	0.00	0.58	0.54	0.23
T16	5	0	0.00	0.70	0.56	0.06

T17	5	0	0.00	0.86	0.75	0.47
T18	5	0	0.00	0.73	0.85	0.40
Total	89	10	11.24			

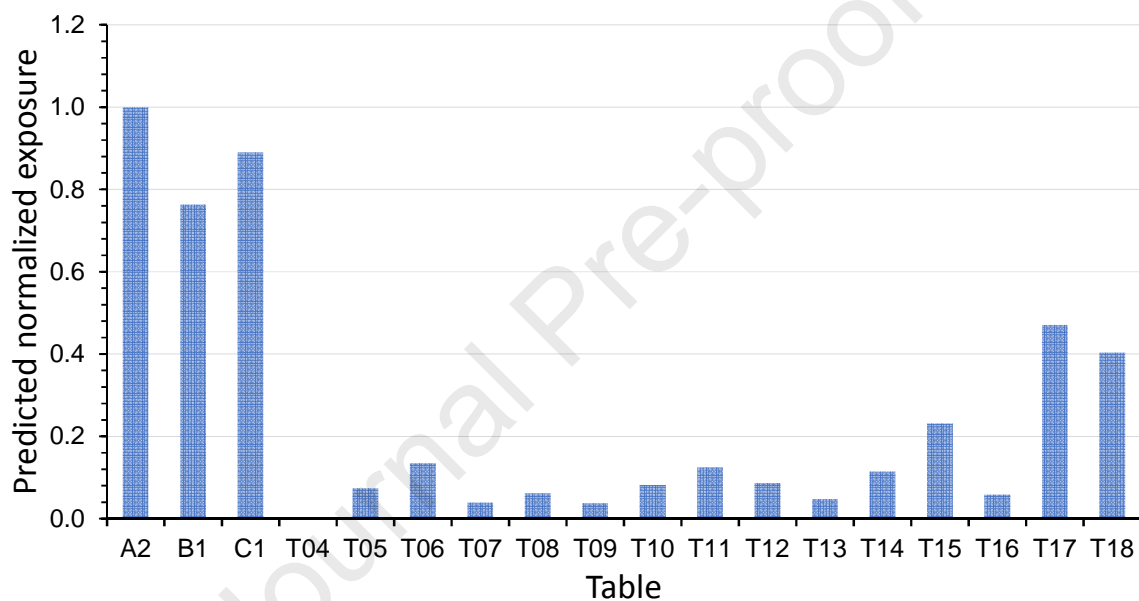
328

329 The formation of a relatively isolated contamination cloud in the ABC zone is supported by
 330 both the measured ethane concentration data and predicted droplet nuclei concentration data.
 331 The average measured ethane concentrations over a period of 66.67 min (Table 3) at TA, TB,
 332 and TC are the highest, being 1.00, 0.92, and 0.96 (normalized by the concentration at TA),
 333 respectively, whereas the concentrations are 0.86 and 0.73 at T17 and T18, respectively, and
 334 0.55–0.70 at the other remote tables. As expected, some mixing clearly occurred between the
 335 different air-conditioning zones (Figure 4), although a stable higher concentration was
 336 maintained in the ABC zone. The predicted normalized ethane concentrations agree well with
 337 the measured values (Figure 5).

338 We use the predicted concentrations of infectious virus-containing droplet nuclei (5 μm) in
 339 the restaurant (Figure 6) to calculate the exposure using the exposure duration data in Table 1.
 340 When the deposition, filtration, and virus deactivation are considered, the predicted
 341 normalized time-averaged concentrations of the infectious virus-containing droplet nuclei (5
 342 μm) during the entire period of TA's presence reveal the additional ABC bubble effect, i.e.
 343 the concentrations at other tables become much lower than those at TA–TC (Figure 7). It
 344 should be noted that if the deposition, filtration, and deactivation were not considered, there
 345 would also be significant exposure for patrons at Table T17 due to their relative long duration
 346 of stay in the restaurant.

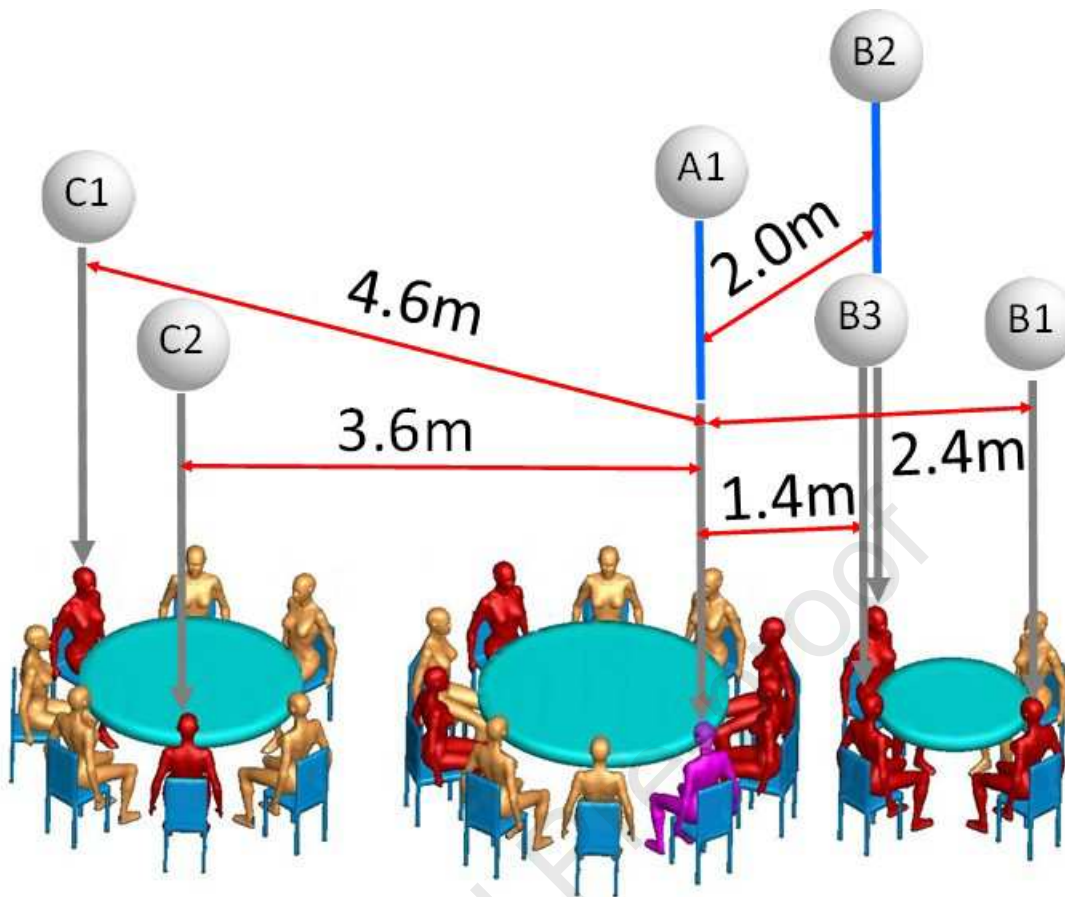
347 The predicted normalized exposure to the exhaled infectious virus droplet nuclei of all tables
 348 are also listed in Table 3. According to the results of the logistic regression model, a higher

349 measured concentration of tracer gas is associated with a higher risk of acquiring COVID-19
 350 (odds ratio associated with a 1% increase in concentration: 1.115; 95% CI: 1.009–1.232; $P =$
 351 0.033) (Table 1). Similarly, a higher predicted concentration of tracer gas and higher
 352 predicted exposure of the infectious virus-containing droplet nuclei ($5\ \mu\text{m}$) are associated
 353 with a higher risk of acquiring COVID-19 (odds ratio associated with a 1% increase in tracer
 354 gas concentration: 1.268, 95% CI: 1.029–1.563, $P = 0.026$; odds ratio associated with a 1%
 355 increase in exposure of droplet nuclei: 1.079, 95% CI: 1.020–1.142, $P = 0.008$).



356

357 **Figure 7.** (Color Online) Predicted exposure of the infectious-virus-containing droplet nuclei
 358 normalized to A1 during the entire lunch period at all tables. As no patron was present at
 359 Table T04, no exposure can be calculated.



360

361 **Figure 8.** (Color Online) Distances between index case A1 (purple) and the five infected
 362 individuals of families B and C (red).

363

364 4. Discussion

365 4.1 Poor ventilation and air distribution led to the outbreak.

366 Lu et al. (2020) suggested that droplet transmission was the most likely primary cause of this
 367 outbreak, but pointed out that the outbreak cannot be explained by droplet transmission alone
 368 because the distances between the index case (A1) and patrons at the other tables are all
 369 greater than 1 m. We estimate that such distances may have been as great as 4.6 m (Figure 8).
 370 The video records also reveal that the index case never turned their head toward TB during
 371 the lunch. Lu et al. (2020) also suggested that “strong airflow from the air conditioner could

372 have propagated droplets from table C to table A, then to table B, and then back to table C,”
373 but stopped short of pinpointing the role of airborne transmission due to the lack of
374 environmental data. The role of airborne transmission was first postulated by the Chinese
375 National Health Commission (NHC) (Li and Gao, 2020) during the early phase of the
376 COVID-19 epidemic in China; however, no specific evidence is provided in the NHC’s
377 recommendation.

378 Our prediction shows that a contaminated recirculation bubble was created in the ABC zone
379 (Figure 3), which sustained a higher concentration of exhaled droplet nuclei from the index
380 case. The formation of individual circulation zones was due to the spatial configuration of the
381 restaurant and interaction of high-momentum air flow of the five air-conditioning units
382 (Figure 4). Within the ABC bubble, the infectious virus-containing droplet nuclei would have
383 had time to be deposited, filtered, and deactivated. This is supported by our computer
384 simulation with a measured filtration efficiency of 20% of the 5- μ m droplet nuclei, which
385 showed that patrons A2, B1, and C2 were exposed to an average concentration of 0.8,
386 whereas patrons at T17 and T19 were only exposed to an average concentration of 0.3. The
387 overlap period for families A and B in the restaurant was 53 min (between 12:01 and 12:54)
388 and 75 min for families A and C (between 12:03 and 13:18), which would have allowed
389 sufficient exposure time to the exhaled droplets. Patient C1 arrived late, at 12:32, and had a
390 46-min overlap with family A. That none of the waiters were infected can be attributed to
391 their relatively short exposure time to exhaled droplets from the index case. A relatively high
392 concentration of tracer gas was also measured at T17 and T18 due to their proximity to the
393 ABC recirculation bubble. Patrons at T17 had only 23 min of overlap with TA but continued
394 to be exposed to the remaining suspended droplet nuclei after family A had left the restaurant.
395 Nevertheless, a low level of exposure to the infectious virus-containing droplet nuclei was
396 predicted because the virus was not only deactivated in aerosols and also removed by

397 deposition and filtration of the air conditioning units as these virus-containing droplet nuclei
398 circulated within the ABC recirculation bubble. None of the patrons at this table ($n = 5$) were
399 infected. Note that additional patrons or restaurant staff may have contracted COVID-19
400 owing to exposure to the virus in Restaurant X but were asymptomatic, however,
401 asymptomatic infection was paid little attention at the time.

402 However, the formation of a contaminated recirculation bubble in the ABC zone cannot alone
403 explain the outbreak. Further evidence comes from the low ventilation rates: the observed
404 high concentrations of the simulated contamination result from the lack of outdoor air supply.
405 The exhaust fans in the walls were found to be turned off and sealed during the January 24
406 lunch, meaning that there was no outdoor air supply aside from infiltration and infrequent and
407 brief opening of the fire door due to the negative pressure generated by the exhaust fan in the
408 restroom. This outdoor air was mainly distributed to the non-ABC zone, thus exacerbating
409 the ventilation deficit of the ABC zone. Ventilation in this study is defined as the supply of
410 outdoor air into the restaurant, and the distribution of the supplied outdoor air in the
411 restaurant. Ventilation is different from air conditioning, however, the supply airflow of the
412 fan coil units, interacting with human body flows, governs the airflow pattern in the
413 restaurant.

414 The measured averaged ventilation rate of 0.90 L/s per patron in the restaurant is
415 considerably lower than the 8–10 L/s per person required by most authorities or professional
416 societies (American Society of Heating, Refrigerating and Air-Conditioning Engineers
417 Standard 62.1, 2019). The restaurant was also crowded and extra tables had been added to
418 accommodate the increased number of customers on Chinese New Year's Eve. Consequently,
419 the occupant density was only 1.55 m² per patron, including the area occupied by tables. The
420 transmission of SARS-CoV-2, which subsequently resulted in an outbreak of COVID-19,
421 thus occurred in a crowded and poorly ventilated space.

422 We also attempted to identify the role of fomite and close contact transmission by examining
423 individual trajectories during the patrons' stay in the restaurant from the available video
424 records. We did not find any evidence to support exposure to SARS-Co-V2 via these routes
425 in this instance.

426

427 More than two thousands of superspreading events or outbreaks of COVID-19 have been
428 documented by Swinkels (2020), who also concluded that “nearly all SSEs [super spreading
429 events] in the database took place indoors.” Qian et al (2020) identified 318 outbreaks each
430 with a minimum of 3 cases, comprising a total of 1245 confirmed cases in 120 prefectural
431 cities in non-Hubei provinces, China, and found that none occurred in outdoor settings. High
432 attack rates of COVID-19 have also been found in choir rehearsal (Charlotte, 2020; Miller et
433 al. 2021), homeless shelters (Imbert et al. 2020; Ralli et al. 2021; Tobolowsky et al. 2020);
434 nightclubs (Kang et al. 2020); Fitness centers (Bae et al. 2020; Jang et al. 2020) and meat
435 processing plants (Günther et al. 2020). Although airborne transmission has been suspected in
436 many of these outbreaks, ventilation rates were not measured in the infection venues.

437 ***4.2 Estimation of quanta generation***

438 Estimation of quanta generation in this outbreak is challenging as the flow is not fully mixed.
439 However, it might still be useful to offer an estimation based on the fully mixing condition.
440 The volume of air in the restaurant is 431 m^3 . The averaged air change rate during two
441 measurements were 0.67 h^{-1} . We adopted an aerosol deposition rate of 0.3 h^{-1} and virus
442 deactivation rate of 0.63 h^{-1} (Miller et al. 2021). The pulmonary flow rate for restaurant
443 setting is $1.65 \text{ m}^3/\text{h}$. As the effective air change rate is only 1.60 h^{-1} , the transient Wells-Riley
444 equation needs to be used, which gives an estimated quanta generation rate of 79.3 quanta/h ,
445 which is compared with $970 \pm 390 \text{ quanta/h}$ in a choir rehearsal outbreak (Miller et al. 2021),

446 about 5.0 quanta/h in light exercise with speaking conditions by Buonanno, et al. (2020), and
447 14-48 quanta/h using a reproductive number-based fitting approach (Dai and Zhao, 2020).
448 According to Sun et al (2020), "...infectiousness profile of a typical SARS-CoV-2 patient
449 peaks just before symptom presentation", which is also supported by other studies (e.g. Cevik
450 et al. 2021; He et al. 2020; Wei et al. 2020). Our estimated relatively large quanta generation
451 rate for the pre-symptomatic index case is also in agreement with this theory of peak
452 infectiousness just before the symptom presentation, as the index case only developed
453 symptoms after the lunch, and she seemed having not infected others elsewhere.

454 To ensure that there is less than one person to be infected in the restaurant, the estimated
455 minimum ventilation rate becomes 38.6 L/s per person using the estimated quanta value. This
456 estimated minimum ventilation rate is much larger than the required minimum ventilation
457 rate of 5.1 L/s per person in restaurants/dining rooms by international ventilation standards
458 such as ASHRAE 62.1 (2019).

459 ***4.3 Importance of sufficiently low occupancy and other intervention***

460 Lack of adequate ventilation and overcrowding is known to be associated with respiratory
461 infection outbreaks, although some are not commonly thought to be transmitted by aerosols.
462 This restaurant SARS-CoV-2 outbreak resembles the Alaska plane influenza outbreak (Moser
463 et al. 1979), in which a plane with a 56-seat passenger compartment was delayed by engine
464 trouble and no mechanical ventilation was provided during the 4.5-h wait. The index case
465 was a passenger who became ill with influenza within 15 min after boarding the plane. There
466 was approximately 3 m³ of compartment space per seat, and the provision of outdoor air was
467 only possible by the plane doors being open for some periods during the 4.5-h wait and
468 during the movement of passengers in and out of the plane. According to Rudnick and Milton
469 (2003), this resulted in there being only 0.08–0.40 L/s of air circulation per passenger, which

470 is slightly less than the range measured in Restaurant X, and this resulted in 72% of the 54
471 passengers on board this plane being infected with influenza.

472 A systematic review by the World Health Organization (WHO) also found evidence for the
473 association between crowding and infection (WHO, 2018). During the 2009 H1N1 pandemic,
474 the basic reproduction number was as high as 3.0–3.6 in outbreaks in crowded schools,
475 compared to 1.3–1.7 in less crowded settings (Lessler et al. 2009; Writing Committee, 2010).
476 The SARS-CoV-2 virus can survive in air for at least 3 h (van Doremalen et al. 2020) and
477 airborne influenza virus genomes and viable influenza virus particles have been detected
478 (Lindsley et al. 2012, 2016; Xie et al. 2020; Yan et al. 2018).

479 It is important to note that our results do not indicate that long-range airborne transmission of
480 SARS-CoV-2 can occur in any indoor space, but rather that transmission may occur in a
481 crowded and poorly ventilated space. Gao et al. (2016) showed that the relative contribution
482 of aerosols to respiratory infection is a function of ventilation flow rate. A sufficiently high
483 ventilation flow-rate reduces the contribution of airborne transmission to a very low level,
484 whereas a low ventilation flow-rate leads to a relatively high contribution of aerosols to
485 transmission. For airborne transmission of respiratory infection such as COVID-19, the
486 infectious virus is carried by aerosols. These aerosols can be not only removed by ventilation,
487 but also by deposition and filtration, and the virus in aerosols can be deactivated, e.g. by
488 ultraviolet germicidal irradiation (UVGI). Therefore, in addition to ventilation, effectiveness
489 of other aerosol removal, and/or virus deactivation methods should be explored.

490 In summary, our epidemiologic analysis, onsite experimental tracer measurements, and
491 airflow simulations support the probability of a long-range aerosol spread of the SARS-CoV-
492 2 having occurred in the poorly ventilated and crowded Restaurant X on January 24, 2020.

493 This conclusion has important implications for intervention methods in the ongoing COVID-
494 19 pandemic. Our study suggests that it is crucial to prevent overcrowding and provide good
495 ventilation and effective air distribution in buildings and transport cabins to prevent the
496 spread of SARS-CoV-2 and the development of COVID-19.

497

498 **Author contributions**

499 Y. Li, H. Qian, J. Hang and M. Kang contributed equally. Y. Li, M. Kang, and H. Qian
500 contributed to the study design, hypothesis formulation, and coordination. H. Qian led the
501 CFD modeling. J. Hang led the field environmental experiments. M. Kang, J. Li, and X. Chen,
502 contributed to the field investigation, data analyses, and reporting. X. Chen, P. Liang, and H.
503 Ling contributed to the field studies and experiments. J. Wei and L. Liu contributed to
504 experimental design. S. Wang contributed to CFD modeling. S. Xiao contributed to the
505 statistical analysis. Y. Li wrote the first draft of the paper. M. Kang, H. Qian, J. Hang, and X.
506 Chen contributed to major manuscript revisions. All of the other authors contributed to
507 revisions.

508

509 **Declaration of Competing Interest**

510 The authors declare no conflict of interest.

511 All of the authors approved the submitted version and have agreed to be personally
512 accountable for their own contributions.

513

514 **Acknowledgments**

515 Funding: This work was supported by the Research Grants Council of Hong Kong's General
516 Research Fund [grant number 17202719]; Research Grants Council of Hong Kong's
517 Collaborative Research Fund [grant number C7025-16G]; the National Key Research and
518 Development Program of China [grant number 2017YFC0702800]; the National Natural
519 Science Foundation of China [grant number 41875015]; and the Science and Technology
520 Planning Project of Guangdong Province [grant number 2019B111103001].

521 The authors are grateful to colleagues at Guangzhou CDC, Guangzhou Yuexiu CDC, and
522 Guangdong CDC who helped in collecting the epidemiologic data, and to Professor Bao
523 Ruoyu and students of Sun Yat-sen University for assisting with the field experiments.

524

525 **References**

- 526 1. American Society of Heating, Refrigerating and Air-Conditioning Engineers (ASHRAE)
527 Ventilation for acceptable indoor air quality. Atlanta, USA: ASHRAE Standard 62.1,
528 2019.
- 529 2. Bae S, Kim H, Jung TY, et al. Epidemiological Characteristics of COVID-19 Outbreak
530 outbreak at Fitness fitness Centers centers in Cheonan, Korea. Journal of Korean medical
531 science, 2020; 35(31):e288.
- 532 3. Bivolarova M, Ondráček J, Melikov A, et al. Comparison between tracer gas and aerosol
533 particles distribution indoors: The impact of ventilation rate, interaction of airflows, and
534 presence of objects. Indoor Air, 2017; 27(6): 1201-1212.
- 535 4. Buonanno G, Stabile L, Morawska L. Estimation of airborne viral emission: quanta
536 emission rate of SARS-CoV-2 for infection risk assessment. Environment International,
537 2020; 141:105794.

- 538 5. Cevik M, Tate M, Lloyd O, et al. SARS-CoV-2, SARS-CoV, and MERS-CoV viral load
539 dynamics, duration of viral shedding, and infectiousness: a systematic review and meta-
540 analysis. *The Lancet Microbe*, 2021;2(1):e13-e22.
- 541 6. Charlotte N. High rate of SARS-CoV-2 transmission due to choir practice in France at the
542 beginning of the COVID-19 pandemic. *Journal of Voice*, 2020.
543 <https://doi.org/10.1016/j.jvoice.2020.11.029>
- 544 7. Dai H and Zhao B. Association of the infection probability of COVID-19 with ventilation
545 rates in confined spaces. *Building Simulation*, 2020; 13:1321–1327.1-7.
- 546 8. Günther T, Czech-Sioli M, Indenbirken D, et al. SARS-CoV-2 outbreak investigation in a
547 German meat processing plant. *EMBO molecular medicine*, 2020; 12:e13296.
- 548 9. He X, Lau EH, Wu P, et al. Temporal dynamics in viral shedding and transmissibility of
549 COVID-19. *Nature Medicine*, 2020; 26(5): 672-675.
- 550 10. Holmberg S and Li Y. Modelling of indoor environment - particle dispersion and
551 deposition. *Indoor Air*, 1998; 8(2): 113-122.
- 552 11. Imbert E, Kinley PM, Scarborough A, et al. Coronavirus Disease 2019 (COVID-19)
553 outbreak in a San Francisco homeless shelter. *Clinical Infectious Diseases*, 2020;
554 ciaa1071..
- 555 12. Jang S, Han SH, Rhee JY. Cluster of coronavirus disease associated with fitness dance
556 classes, South Korea. *Emerging infectious diseases*, 2020; 26(8): 1917.
- 557 13. Kang CR, Lee JY, Park Y, et al. Coronavirus disease exposure and spread from
558 nightclubs, South Korea. *Emerging infectious diseases*, 2020; 26(10): 2499.
- 559 14. Lessler J, Reich NG, Cummings DA, et al. Outbreak of 2009 pandemic influenza A
560 (H1N1) at a New York City school. *New England Journal of Medicine*, 2009; 361(27):
561 2628-2636.

- 562 15. Li X and Gao F. Public Prevention Guidelines of Infection due to the Novel Coronavirus
563 Pneumonia (In Chinese, 新型冠状病毒感染的肺炎公众防护指南). Beijing, China:
564 People's Medical Publishing House, 2020; 9.
- 565 16. Li Y, Huang X, Yu ITS, et al. Role of air distribution in SARS transmission during the
566 largest nosocomial outbreak in Hong Kong. *Indoor Air*, 2005; 15: 83-95.
- 567 17. Lindsley WG, Blachere FM, Beezhold DH, et al. Viable influenza A virus in airborne
568 particles expelled during coughs versus exhalations. *Influenza and other respiratory*
569 *viruses*, 2016; 10: 404-413.
- 570 18. Lindsley WG, Pearce TA, Hudnall JB, et al. Quantity and size distribution of cough-
571 generated aerosol particles produced by influenza patients during and after illness. *Journal*
572 *of occupational and environmental hygiene*, 2012; 9(7): 443-449.
- 573 19. Lu J, Gu J, Li K, et al. COVID-19 outbreak associated with air conditioning in restaurant,
574 Guangzhou, China. *Emerging infectious diseases*, 2020; 26(7): 1628.
- 575 20. Miller SL, Nazaroff WW, Jimenez JL, et al. Transmission of SARS-CoV-2 by inhalation
576 of respiratory aerosol in the Skagit Valley Chorale superspreading event. *Indoor Air*,
577 2021; 0031: 3141-32310.
- 578 21. Miller SL, Nazaroff WW, Jimenez JL, et al. Transmission of SARS-CoV-2 by inhalation
579 of respiratory aerosol in the Skagit Valley Chorale superspreading event. *Indoor air*, 2020.
- 580 22. Morawska L and Cao J. Airborne transmission of SARS-CoV-2: The world should face
581 the reality. *Environment International*, 2020; 139:105730.
- 582 23. Moser MR, Bender TR, Margolis HS, et al. An outbreak of influenza aboard a
583 commercial airliner. *American journal of epidemiology*, 1979; 110(1): 1-6.
- 584 24. Qian H, Miao T, Li LIU, et al. Indoor transmission of SARS-CoV-2. *Indoor Air*, 2020.

- 585 25. Ralli M, Morrone A, Arcangeli A, et al. Asymptomatic patients as a source of
586 transmission of COVID-19 in homeless shelters. *International Journal of Infectious*
587 *Diseases*, 2021;103:243-245.
- 588 26. Riley EC, Murphy G, Riley RL. Airborne spread of measles in a suburban elementary
589 school. *American Journal of Epidemiology*, 1978; 107(5): 421-432.
- 590 27. Rudnick SN and Milton DK. Risk of indoor airborne infection transmission estimated
591 from carbon dioxide concentration. *Indoor Air*, 2003; 13(3): 237-245.
- 592 28. Sun K, Wang W, Gao L, et al. Transmission heterogeneities, kinetics, and controllability
593 of SARS-CoV-2. *Science*, 2021;371:254-2540.
- 594 29. Swinkels, K. (2020). SARS-CoV-2 Superspreading events around the world.
595 <https://kmswinkels.medium.com/covid-19-superspreading-events-database-4c0a7aa2342b>.
596 Accessed on 29 December 2020. [dataset]
- 597 30. Tobolowsky FA, Gonzales E, Self JL, et al. COVID-19 outbreak among three affiliated
598 homeless service sites-King County, Washington, 2020. *Morbidity and Mortality Weekly*
599 *Report*, 2020; 69(17): 523.
600 Updated on 28 October 2020. (Accessed on 15 November 2020).
- 601 31. US Centers for Disease Control and Prevention (CDC). Scientific Brief: SARS-CoV-2
602 and Potential Airborne Transmission. [https://www.cdc.gov/coronavirus/2019-ncov/more/](https://www.cdc.gov/coronavirus/2019-ncov/more/scientific-brief-sars-cov-2.html)
603 [scientific-brief-sars-cov-2.html](https://www.cdc.gov/coronavirus/2019-ncov/more/scientific-brief-sars-cov-2.html). Updated on 5 October 2020. (Accessed on 15 November
604 2020).
- 605 32. USA Centers for Disease Control and Prevention (CDC). How 2019-nCoV spreads.
606 Washington DC, USA: U.S. Department of Health & Human Services, 2020.
607 <https://www.cdc.gov/coronavirus/2019-ncov/about/transmission.html>

- 608 33. van Doremalen N, Morris DH, Holbrook MG, et al. Aerosol and surface stability of
609 SARS-CoV-2 as compared with SARS-CoV-1. *New England Journal of Medicine*, 2020;
610 382(16): 1564-1567.
- 611 34. Wei WE, Li Z, Chiew CJ, et al. Presymptomatic Transmission of SARS-CoV-2-
612 Singapore, January 23-March 16, 2020. *Morbidity and Mortality Weekly Report*, 2020;
613 69(14): 411.
- 614 35. Wong TW, Li CK, Tam W, et al. Cluster of SARS among medical students exposed to
615 single patient, Hong Kong. *Emerging infectious diseases*, 2004; 10: 269-276.
- 616 36. World Health Organization. Coronavirus disease (COVID-19): How is it transmitted?
617 [https://www.who.int/news-room/q-a-detail/coronavirus-disease-covid-19-how-is-it-](https://www.who.int/news-room/q-a-detail/coronavirus-disease-covid-19-how-is-it-transmitted)
618 [transmitted](https://www.who.int/news-room/q-a-detail/coronavirus-disease-covid-19-how-is-it-transmitted). Updated on 9 July 2020. (Accessed on 15 November 2020).
- 619 37. World Health Organization. WHO housing and health guidelines.
620 <https://www.who.int/sustainable-development/publications/housing-health-guidelines/en/>.
621 Updated on 23 November 2018. (Accessed on 15 November 2020).
- 622 38. Writing Committee of the WHO Consultation on Clinical Aspects of Pandemic (H1N1)
623 2009 Influenza. Clinical aspects of pandemic 2009 influenza A (H1N1) virus infection.
624 *New England Journal of Medicine*, 2010; 362(18): 1708-1719.
- 625 39. Xie C, Lau EH, Yoshida T, et al. Detection of influenza and other respiratory viruses in
626 air sampled from a university campus: a longitudinal study. *Clinical Infectious Diseases*,
627 2020; 70(5): 850-858.
- 628 40. Yan J, Grantham M, Pantelic J, et al. Infectious virus in exhaled breath of symptomatic
629 seasonal influenza cases from a college community. *Proceedings of the National*
630 *Academy of Sciences*, 2018; 115: 1081-1086.
- 631 41. Yu ITS, Li Y, Wong TW, et al. Evidence of airborne transmission of the severe acute
632 respiratory syndrome virus. *New England Journal of Medicine*, 2004; 350: 1731-1739.

634 **Appendix A: Basic patient information**635 **Table A.1** Basic patient information.

Case	Family data	Basic data	Symptom onset date	Symptoms	Confirmation date
A1	Residents of Wuhan, arrived in Guangzhou on Jan. 22. Family A	female, 63 y.o., history of hypertension, hyperlipidemia, and cervical spondylosis.	Jan. 24	Fever (37.5 °C), dry cough	Jan. 26
A2	includes four small families: the family of the index case including their	female, 60 y.o., younger sister of case A1, was in good health.	Jan. 27	Fever (37.8 °C)	Jan. 27
A3	husband and grandson ($n = 3$); mother-in-law's family ($n = 2$); sister's	female, 62 y.o., mother-in-law of A1's son, was in good health.	Jan. 29	Fever (37.3 °C)	Jan. 30
A4	family ($n = 2$); and niece's	female, 34 y.o., niece of A1, was in good health.	Jan. 29	Fever (not recorded)	Jan. 30
A5	family ($n = 3$)	male, 63 y.o., father-in-law of A1's son, was in good health.	Feb. 2	Fever (not recorded)	Feb. 3

B1	Residents of Guangzhou.	female, 44 y.o., was in good health.	Feb. 1	Fever (38.4 °C), cough, sputum	Feb. 4
B2	Family B ($n = 4$) includes one family, although the older mother lived alone.	female, 20 y.o., daughter of B1, was in good health.	Feb. 3	diarrhea and fever (38.6 °C), dry cough, chest tightness, asthma	Feb. 6
B3		male, 53 y.o., husband of B1, was in good health.	Feb. 5	headache, chest tightness, chest pain, bloating	Feb. 6
C1	Residents of Guangzhou. Family C	female, 82 y.o., retired, was in good health.	Jan. 27	Fever (37.8 °C), runny nose, cough, sputum	Feb. 10
C2	includes three small families: the patient couple and mother ($n = 3$); their son's family ($n = 2$); and brother's family ($n = 2$).	female, 54 y.o., daughter of C1, was in good health.	Jan. 31	fever (39.9 °C), dry cough	Feb. 6

636

637

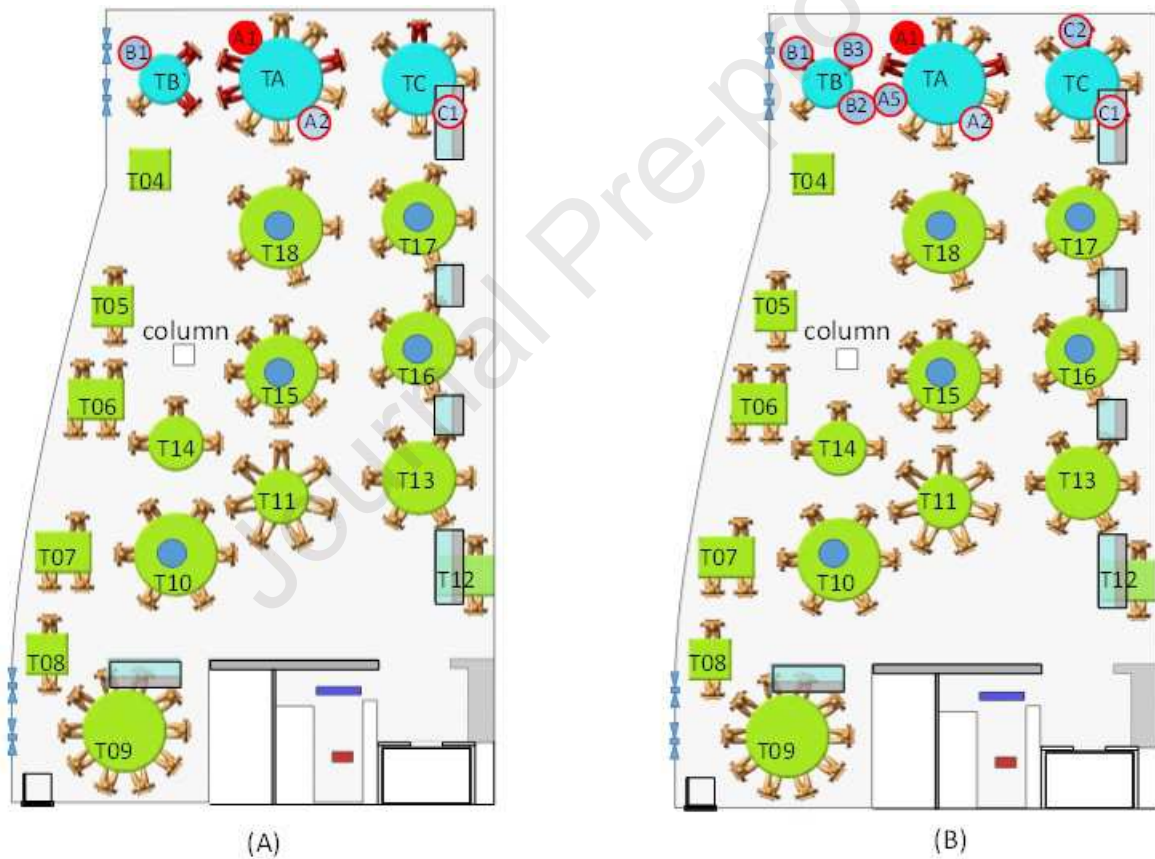
638 **Appendix B: Airflow and dispersion video**

639 **Movie B.1** Spread of exhaled droplet nuclei in the restaurant as predicted by computational
 640 fluid dynamics. Red indicates the highest concentrations and blue the lowest. (see file: Movie
 641 mp4- Spread of exhaled tracer gas in Restaurant X.mp4)

642

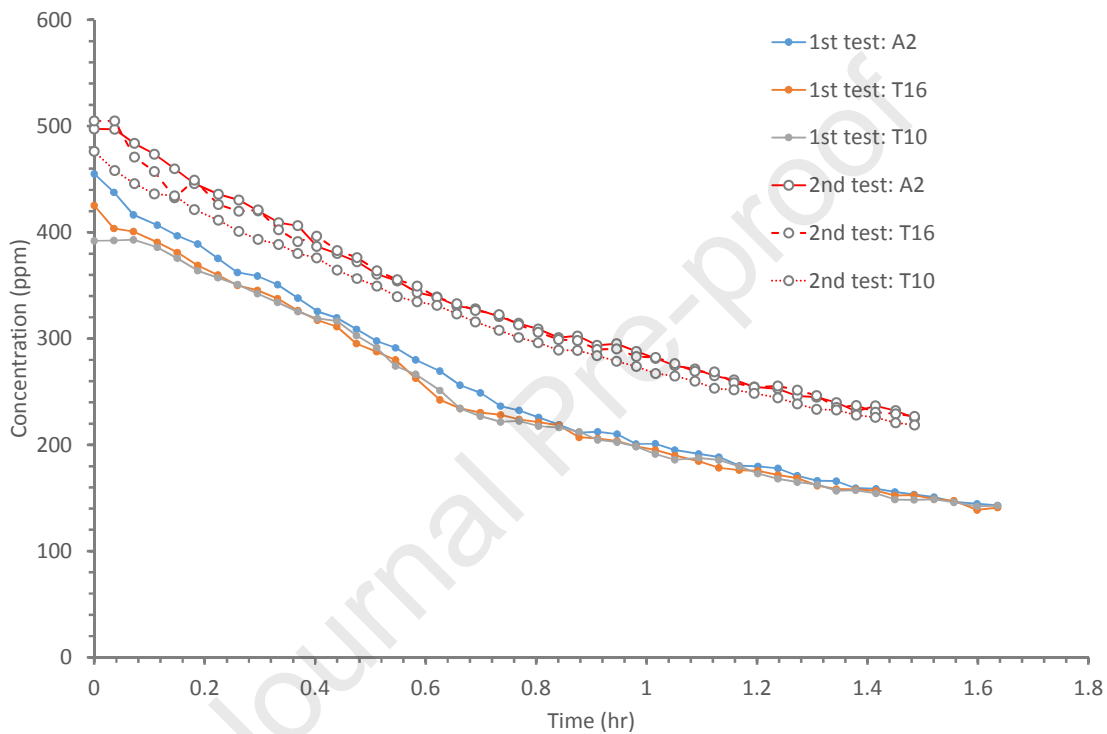
643 **Appendix C: Some measurement details**

644



650 are numbered TA, TB, and TC for families A, B, and C, respectively, and T04–T18 for the
 651 other tables. The morning test with a leak was unintended; the tracer gas leaked due to a
 652 damaged pipe below TA. Nevertheless, the measured data from test (B) also support the
 653 observed distribution in test (A).

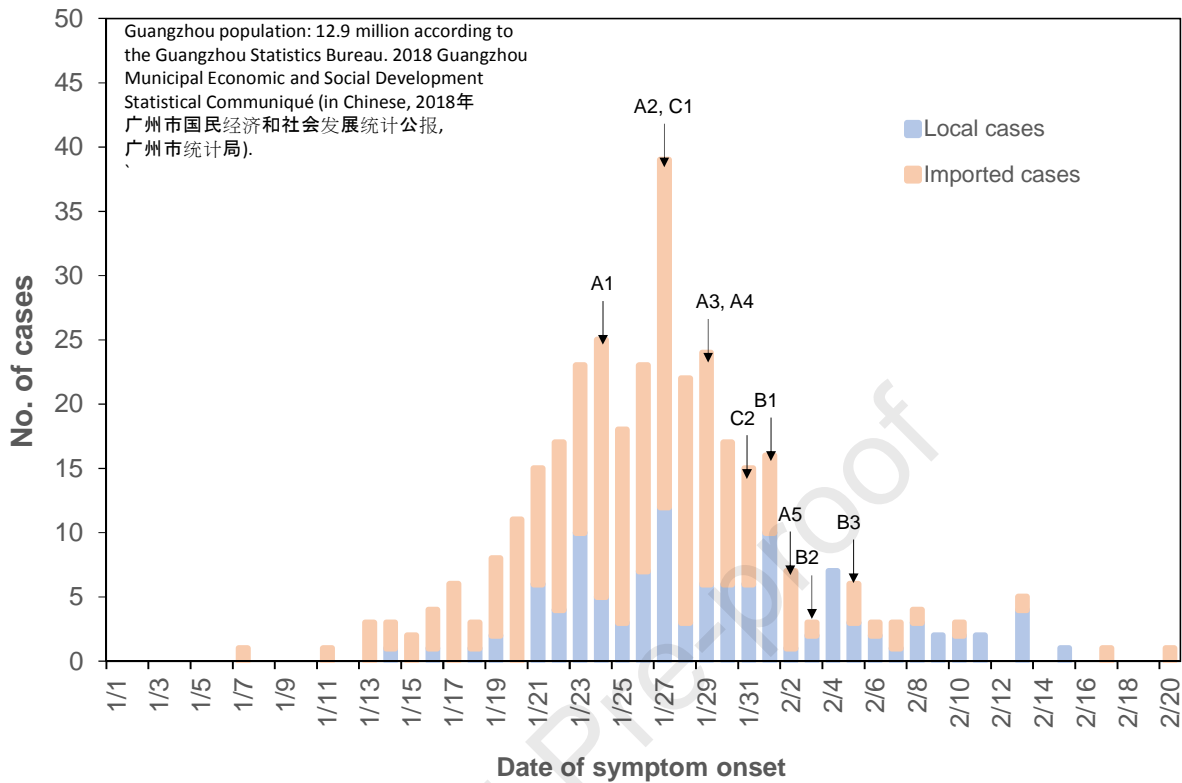
654



655

656 **Figure C.2** (Color Online) Measured tracer gas concentration profile from the two tracer gas
 657 decay tests for ventilation rate measurement. The concentrations were monitored at three
 658 locations during each test: seat A2, Table 10 (T10), and Table 16 (T16). For each test, the
 659 three curves are reasonably close, suggesting the room air flow was reasonably fully mixed
 660 by using the mixing fans during the test.

661

662 **Appendix D: Guangzhou epidemiological data**

663

664 **Figure D.1** (Color Online) The epidemiological curve in Guangzhou (population 12.9
 665 million), where restaurant X is located and where families B and C live. The symptom onset
 666 dates of all infected members of families A, B, and C are also shown. By January 24, when
 667 A1 had the first symptoms, there were 72 symptomatic cases (15 local and 59 imported); by
 668 January 27, when C1 had the first symptoms, there were 202 symptomatic cases (52 local and
 669 150 imported); and by Feb 1, when B1 had the first symptoms, there were 296 symptomatic
 670 cases (83 local and 213 imported). With close contact tracing, families B and C did not have
 671 contact with any of the identified cases and/or any visitors from Hubei Province 14 days prior
 672 to the onset of their symptoms.

Highlights

This outbreak involved ten infected persons in three families;

Full video recording at time of infection allows restoration of the scene;

Time-averaged ventilation rates were only 0.9 L/s per person in the restaurant;

Insufficient ventilation played a role in this outbreak of COVID-19.

Journal Pre-proof

Declaration of interests

The authors declare that they have no known competing financial interests or personal relationships that could have appeared to influence the work reported in this paper.

The authors declare the following financial interests/personal relationships which may be considered as potential competing interests:

Journal Pre-proof